ICES C.M. 1996

PAPER
S:7 - Theme Session S

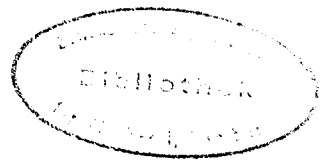

A NUMERICAL MODEL SYSTEM OF THE REGION AROUND THE IBERIAN PENINSULA: MODEL VALIDATION AND APPLICATION TO HAKE LARVAE DRIFT IN THE BAY OF BISCAY

Joachim Bartsch, Alicia Lavín and Lorenzo Motos

ABSTRACT

Within the EU funded SEFOS project (Shelf Edge Fisheries and Oceanography Studies) a numerical model system consisting of a circulation and transport model has been used to model the dispersion of hake eggs and larvae (*Merluccius merluccius*). The area of the model system ranges from Northwest Africa to the northern Bay of Biscay and covers the shelf edge and adjacent waters with a horizontal resolution of 10' × 10'. The circulation model was run using tidal forcing, climatological density fields as well as realistic six-hourly wind stress fields for 1994 and 1995. Current meter data collected in the Cantabrian Sea in the mixed layer and the upper part of the North Atlantic Central Water is used for model validation. Simulated currents from the circulation model were found to be in good agreement with observed current data on the shelf and in the vicinity of the shelf edge. Simulated currents are used as input to the transport model. Egg and larval data used in the dispersion simulation was collected on two cruises carried out in February and March 1995. Horizontal distributions of stage I eggs were used as the initial distribution for the dispersion scenario. Tracers were dispersed in the depth range 50 - 150m for 39 days. Based on estimated egg development times and larval growth rates, stage I eggs will have grown into 6mm larvae in approximately 39 days. The tracer distribution after dispersion from 17 February to 27 March is compared to the distribution of 6mm larvae observed between 22 - 27 March 1995. Agreements and discrepancies between observations and model results are discussed.

Keywords: Numerical model system, model validation, larvae dispersion

Joachim Bartsch: Biologische Anstalt Helgoland, Notkestr. 31, 22607 Hamburg, Germany (tel: 49 40 89693 177, fax: 49 40 89693 115, e-mail: bartsch@ifm.uni-hamburg.de).
Alicia Lavín: Centro Oceanografico de Santander, Apdo 240, 39080 Santander, Spain (tel: 34 42 275033, fax: 34 42 275072, e-mail: lavina@ccaix3.unican.es).
Lorenzo Motos: AZTI, Food and Fish Technological Institute, Avda. Satrustegui 8, 20008 San Sebastian, Basque Country, Spain (tel: 34 43 214124, fax: 3443212162, e-mail: lorenzo@rp.azti.es).

1. INTRODUCTION

One of the specific objectives of the SEFOS (Shelf Edge Fisheries and Oceanography Studies) project is to gain information on the transport patterns of the eggs and larvae of the target species in the SEFOS area. In this investigation *Merluccius merluccius* is considered. To study the drift of eggs and larvae over weeks and months numerical model systems are needed. Only they can provide the variable circulation field over these time spans with the required spatial and temporal resolution. Current data from field surveys and moorings are too sparse to accomplish this. Examples of such modelling drift studies are those carried out in the Gulf of Alaska Shelf area on Walleye Pollock (Stabeno et al., 1995), in the Georges Bank area on Cod and Haddock (Werner et al., 1993) and in the German Bight on Sprat (Bartsch, 1994a and b).

The oceanographic and biological data collected during SEFOS in the Bay of Biscay is used to validate the circulation model and to test the predictive hindcast ability of the model system.

2. THE CIRCULATION AND TRANSPORT MODEL SYSTEM

A three dimensional nonlinear baroclinic numerical model is used to simulate the circulation in the region around the Iberian Peninsula, the shelf edge area and adjacent oceanic regions. The circulation model is based on HAMSOM (HAMburg Shelf Ocean Model) which was developed at the Institut für Meereskunde, Hamburg and was transferred to the southern SEFOS area. No details of the model will be given here, as these have been published elsewhere (Backhaus, 1985).

The model area reaches from 33°N to 47°N and from 15°W to 1°W (fig. 1). The horizontal grid resolution is 10'×10', i.e. 13 km (east-west) by 18.5 km (north-south) in the Bay of Biscay. The vertical resolution consists of 16 layers, with layer depths ranging from 10 m to 40 m in the upper 100 m and increasing steadily in the lower layers. The model is forced by the M_2-tide, six hourly wind stress fields from ECMWF (European Centre for Medium-Range Weather Forecasting) as well as monthly climatological density fields which are treated prognostically but which are relaxed towards the climatological monthly mean.

The time step of the circulation model is 45 min. Due to the high data storage requirements, the current data, as well as the variance of the current was only output on a daily basis, i.e. the currents were integrated over two M_2 - tidal cycles. The daily three dimensional current and variance fields serve as input to the transport model. To elucidate the configuration of the model system, a schematic diagram is given in fig. 2.

The simulations of the drift routes are performed by means of tracers, in essence "marked" water particles which are introduced into the model area and are pursued in the space and time domain. A simple method with which the transport of substances

(particles) can be simulated is the Monte - Carlo method (Bork and Maier - Reimer, 1978). It is assumed that the current field can be split into a large scale mean current ($\overline{u}$) and a small scale random fluctuation (u'), i.e. $u = \overline{u} + u'$. The small scale fluctuations are parameterised using the current variance (Backhaus, 1989; Bartsch, 1994a). Thus, at each timestep, the particle experiences a directional transport by the mean current (advection) as well as a random transport, in magnitude and direction, by the small scale fluctuations (diffusion).

The boundary conditions in the transport model prescribe a no - flux condition at closed boundaries, whereas the tracers may leave the model area at open boundaries. The model area, grid size and the vertical resolution are in accordance with that of the circulation model, while the time step of the transport model is three hours.

3. MATERIALS AND METHODS

(a) CURRENT METER DATA

Within the SEFOS project current data from three moorings were collected for the duration of one year. Data from the upper layers and from the first deployment period from 19 February to 15 May 1995 were used for model validation. Due to the fishing effort in the area and based on previous experience, moorings were placed in the locations shown in fig. 3. The current meter on the shelf was deployed at 75 m depth, which is below the depth of nets used to catch pelagic fish. At the shelf break (mooring 2) the shallow current meter was deployed to study the mixed layer and the second at 180 m to study the upper part of the North Atlantic Central Water.

Moorings were deployed from the B/O Francisco Navarro. CTD profiles were collected during the deployment to observe the hydrographic conditions of the area with the aim of studying the influence of the wind stress on the stratification of the upper layer. In March-April and May-June 1995 two oceanographic SEFOS cruises were carried out in the Cantabrian Sea covering the area in the vicinity of the current meters (Porteiro et al, 1996).

The original current meter time series were obtained with a sampling interval of 30 min. To obtain a preliminary smoothing a Godin A2 A2 A3 filter was used, which effectively eliminated the high frequency noise. The data was filtered again to eliminate the effect of the M_2-tide. This filtering was carried out with a Godin A24 A24 A25 filter with a cut off period of 25 hours (Godin, 1991; Alonso and Diaz del Rio, 1996). After filtering the data was available once an hour.

(b) HAKE EGG AND LARVAL SURVEYS

Data on distribution and abundance of hake eggs and larvae were collected during two consecutive plankton cruises carried out with RV Investigador in the time periods 15-24 February and 22-30 March 1995, respectively. The cruises were specifically designed to establish the horizontal and vertical distributions of hake eggs and larvae together with complementary hydrographical observations at two consecutive times T1 and T2.

Both cruises covered similar areas of the Bay of Biscay (fig. 4), i.e. from the Spanish coast in the south up to 47° 30' N and from the 100 m isobath in the east to 20-30 nautical miles beyond the shelf edge in the west. Both areal coverage and timing of the cruises were determined according to previous work in the area and a literature review (Casarino and Motos, 1994) with the aim of covering a main area of adult hake distribution at the peak of the spawning period.

A detailed report on the methods used during the cruises is given in Motos et al. (1996). The horizontal distribution of hake eggs and larvae was determined from samples collected by oblique BONGO (60 cm diameter) net hauls (Smith and Richardson, 1977). These samples were collected between 16 - 22 February and 22 - 27 March respectively. The vertical distribution was derived from samples collected at selected stations by 1 m^2 mouth aperture ring net hauls. This net was furnished with a double aperture/closure mechanism allowing for the sampling of discrete layers.

Plankton samples were fixed immediately after the completion of the haul in a buffered commercial formaldehyde solution on tap water (10%). All fish eggs and larvae were sorted from the plankton samples in the laboratory. Hake eggs and larvae were identified (Porebsky, 1975; Coombs, 1994; Marrale et al., 1996; Russell, 1978), counted and classified by developmental stage (Coombs and Mitchell, 1982). Larvae were measured (SL) to the lower 0.1 mm. No correction was made to allow for shrinkage of larvae due to fixation procedures. Bailey (1981) gave a shrinkage figure of 9-22% for small Pacific hake larvae (< 4 mm) fixed 5-10 minutes after collection, and he assumed smaller shrinkage rates for bigger larvae. Egg and larval abundances per haul were transformed to densities (numbers per 10 m^2) using standard procedures (Smith and Richardson, 1977).

Temperature, time and depth profiles were recorded by a MINILOG VEMCO data logger in all plankton tows. CTD SEABIRD 25 profiles of temperature, conductivity, turbidity and clorophyll a were collected at selected stations (fig. 4). Unfortunately, the CTD was not deployed during the February cruise due to rough sea conditions.

(c) EGG DEVELOPMENT AND GROWTH RATES

Data on temperature related developmental rates of hake eggs and yolk sac larvae are available in the literature (Coombs and Mitchell, 1982; Marrale et al., 1996). However, no data is available on growth rates of post-larvae of the European hake, neither from our cruise nor from the literature. Alternatively, we used the only available larval growth data for the genus Merluccius, i.e. data from Merluccius productus, a hake species inhabiting waters in the Northeastern Pacific Ocean (Bailey, 1981; Bailey et al.,1982).

According to Coombs and Mitchell (1982) the time necessary for eggs to reach the end of stage IV is identical to the incubation time (duration from spawning to hatching). This ranges from 6.82 to 5.27 days at 10 °C and 12 °C, respectively.

Data on growth rates of yolk-sac larvae is also available. Fig. 2 of Coombs and Mitchell (1982) showed pictures of different stages of yolk-sac larva reared at different temperatures. An early stage at 8.1°C, a mid stage at 10.0°C, a late stage at 15.6°C, and a very late one at 15.6°C. They assign to these stages ages from hatching to fertilization of 200, 191, 177 and 191 hours, respectively. Marrale et al., (1996) incubated hake eggs and yolk-sac larvae from an artifical fertilization experiment. They observed that the development of yolk-sac larvae from hatching to the exhaution of the yolk lasted around 84 hours at 17°C.

In order to have some idea of the actual growth rates of post-larvae of M. merluccius, the available information regarding other Merluccius species was reviewed. Bailey (1981) presented development and growth rates of eggs, yolk-sac larvae and post-larvae of the Pacific hake, Merluccius productus. The results are summarized in tab. 1. Egg development rates are slower in the European hake than in the Pacific hake. These slower development rates may also hold during the larval stages. Assuming similar growth patterns for yolk-sac larvae of both species, the end of this stage at 12 °C would be reached one day later in M. merluccius, when they are $\sim$ 12 days old.

Using the (post) larval growth rates given in tab. 1 for M. productus and the lengths at the beginning of the postlarval stage (1.72 mm for the Gompertz fit and 2.75 mm for the lineal fit), it would take about 31 days (Gompertz fit) or 32 days (Linear fit) to reach a length of 6 mm. Similarly, it would take between 34 (Gompertz fit) to 38 days (Linear fit) to reach 7 mm. Assuming further, that M. merluccius larvae have slower growth rates than their pacific counterparts, it is probable that the stage I eggs on cruise 1 (around 17 February) developed into 6 mm larvae by cruise 2 (around 27 March) at a temperature of $\sim$ 12 °C, i.e. during 39 days.

4. RESULTS

(a) CURRENT OBSERVATIONS

The meteorological conditions over the Bay of Biscay during the sampled period are characterised by a continuous track of high and low pressure cells (Instituto Nacional de Meteorologia, 1995). These conditions produce NW, SW and NE winds as well as relaxed periods. There were two periods with a high pressure cell remaining over the area for longer periods, one in late March and the other during the first half of April. In these periods NE winds dominated the meteorological conditions over the Bay of Biscay.

Current meter mooring 3 lies on the shelf in water 90 m deep. The observed time series for this current meter, deployed at 74m, is given in fig. 5a. Over the shelf, currents were oscillatory NW/SE with periods around 8 - 10 days. Mean values of the east and north components were 0.42 cm/s and -0.47 cm/s, and maximum values were 13 cm/s and - 4.5 cm/s respectively for the period.

Mooring 2 was deployed at the shelf edge in a water depth of 568 m. The top current meter at mooring 2 was deployed at 75m and the time series is given in fig. 6a. At the beginning of the sampling period, currents were mainly eastward, corresponding to the winter circulation in the southern Bay of Biscay. Around the middle of March, the mean direction of the current reversed and now showed westward flow, which is usually observed during spring and summer (Pingree and Le Cann, 1990; Diaz del Rio et al., 1992; Porteiro et al., 1996). Mean values for the east and north components were -3.2 cm/s and -3.5 cm/s, and maximum values were -18 cm/s and -12 cm/s respectively for the period.

The second current meter at mooring 2 was deployed at 180m depth and the time series is given in fig. 7a. The current was predominantly eastward throughout the period and only at the end of March and at the end of April westward directed currents were observed. Mean values for the east and north components were 1.7 cm/s and -2.5 cm/s, and maximum values were - 12 cm/s and -9 cm/s respectively for the period.

In this area of the Bay of Biscay, density gradients are very small and wind stress is the main forcing factor of circulation in the area. The x-component of the wind stress seems to be correlated to east component of the current in the mixed layer. Over the continental shelf salinity stratification was observed in winter and during spring salinity and temperature stratification was observed above the upper current meter. Intensification of the currents in the central period could be due to a lack of stratification.

At the shelf break at the beginning of the sampling period the upper 200 m of the water column was nearly homogeneous, but in May waters in the vicinity of moorings 2 and 3 were stratified. Westward currents are forced by a high

pressure cell over the Bay of Biscay. If the situation is not persistent, as was the case around February 28 and March 12, a pulse of westward current of 12 cm/s or 14 cm/s at 75 m depth and weaker currents at 180 m depth were observed. If the high pressure cell is persistent, westward flow persists over the period at 75 m depth as was the case in the second half of March and April with some fluctuations in intensity, and reduced westward flow is found at 180 m depth.

(b) MODEL VALIDATION

The horizontal model grid resolution is 13 × 18.5 km in the Bay of Biscay. Simulated current data is taken from that model grid box which encompasses the area in which the current meter mooring was deployed. The appropriate layer is chosen in accordance with the depth of the current meters. Model data is available once a day and was extracted at the specific grid points and layer depths. Time series were constructed for the period February to May 1995 and were compared to the observed current time series.

The modelled time series for mooring 3 is given in fig. 5b. It can be seen that modelled currents speeds often underestimate observed current speeds. Current fluctuations in the u - component (east - west) are reproduced by the model, although peaks do not always coincide. Simulated current variability in the v - component (north - south) is reduced compared to the observations.

The corresponding model time series (model layer 5) for mooring 2, top current meter is shown in fig. 6b. Again current speeds are generally underestimated by the model both in the u- and especially the v - components. Current fluctuations are reproduced by the model and usually peaks in current speeds between observations and simulations coincide.

The model time series (model layer 7) for mooring 2, bottom current meter is shown in fig. 7b. Modelled and observed time series show many similarities for this current meter. Maximum observed current speeds are $\sim$ 12 cm/s while maximum modelled current speeds are $\sim$ 10 cm/s. Current variability is similar for observation and simulation both for the u- and v-component and usually current speed peaks coincide.

(c) HAKE EGG AND LARVAE DISTRIBUTIONS

Figs. 8a and 8b show the distribution of stage I hake eggs on the first cruise and 6 mm larvae on the second cruise respectively. Both larval and egg abundances were an order of magnitude higher in March than they were in February showing that the second cruise was closer to the seasonal spawning peak.

In February, stage I eggs were found in two patches (Fig. 8a). A bigger patch extended from 45° N to 46° N having lower abundances on the central transect. Eggs were more abundant over the shelf edge both in the northern and in the southern tips of the patch and extended over the outer platform (100-200 m)

in the northern and southern parts. Another, smaller patch was located in the southeastern corner of the Bay of Biscay (eastern Cantabrian Sea).

The second cruise started on 22 March, 29 days after the end of the first one, and was completed on 30 March. Larvae bigger than 6 mm SL appear in two areas (Fig. 8b). A more extensive one in the northern part of the sampling area, from 46° to 47° 15' N, with main abundances around 47° N over the shelf edge and 20-40 miles off the shelf edge. This patch extended further to the south down to 46° N over shelf waters 100-200 m deep. A second, smaller patch was observed in the southeastern corner of the Bay of Biscay.

(d) TRACER SIMULATIONS

Currents in the region around the Iberian Peninsula were simulated for 1994 and 1995. The simulated currents as well as the daily variance of the currents for February and March 1995 served as input to the transport model. An example of the circulation field on 10. 3. 1995 in model layers 5 and 6 is given in figs. 9a and 9b.

A simplified scheme of vertical distributions of hake eggs and larvae in the Bay of Biscay based on the field data collected in the February and March cruises was used in the transport model. As most eggs and larvae were found in the depth range of 50 - 150m (Motos et al., 1996), the tracers migrated randomly in this depth range, i.e. tracers spend an equal amount of time in the model layers between 60 - 150m. The tracers thus feel the combined effect of the currents in this depth range. This random migration is not light dependent as the vertical distribution of hake eggs and larvae was similar during night and day.

The distribution of stage I eggs around 17 February (fig. 8a) was interpolated onto the model grid (fig. 10a) and served as the initial distribution for the dispersion simulation. The simulation was begun on 17 February as practically all stage I eggs were caught on 17 and 18 February. The 6 mm hake larvae collected on the second cruise bewteen 22 - 27 March (fig. 8b) was interpolated onto the model grid (fig. 10b) and served as the final distribution for comparison with the dispersion simulation. The dispersion simulation was terminated on 27 March as most 6 mm larvae were caught on 26 and 27 March, except for those in the southeastern corner of the Bay of Biscay which were caught on 22 March.

This cruise survey design enabled the testing of the transport model by using the distribution of stage I eggs at time T1 as initial distribution, simulating for 39 days and comparing the resulting tracer distribution at time T2 with the 6 mm larvae distribution actually found during the second cruise.

Tracers were introduced into the model domain at the appropriate points given by the interpolated egg distribution in fig. 10a in the depth range 60 - 150m on 17 February. Low concentrations are in yellow and the highest concentrations are in violet. Three distinct areas of high stage I egg concentrations can be seen. The northern and central (at 45°) areas lie close to the shelf edge. The central patch

with the highest concentrations lies further off shelf than the northern patch. Another patch with lower concentrations than the other two is evident in the southeastern corner of the Bay of Biscay.

The interpolated larvae distribution of the 6mm length class given in fig. 10b shows six areas of higher concentrations w.r.t. the surrounding areas. The highest concentration was found in the north at 46 ° 30' N and 5 ° W and was situated off-shelf in deeper water (2000 - 3300 m). Another high concentration patch was found in the southeastern corner of the Bay of Biscay. Four smaller, lower concentration patches were found along the shelf edge, situated in a band stretching from 46 ° 50' N southeastward to 45 ° 40' N on the shelf side in water between 100 - 200m deep.

The tracer distribution after 39 days dispersion is given in fig. 10c. Five areas of higher concentration w.r.t. the surrounding areas can be seen in the distribution. The highest concentrations were found at the shelf edge at 45° 20' N and in the southeastern part of the Bay of Biscay. Three areas of higher concentration can be seen aligned along the shelf edge on the shelf side from 46° 30' N to 45° 40' N.

Comparing the simulated distribution (fig. 10c) to the observed larvae distribution (fig. 10b) it is evident that there are two main discrepancies. The observed high concentration of larvae in the north at 46 ° 30' N and 5 ° W is not evident in the modelled distribution. Secondly the high simulated tracer concentration at the shelf edge (at 45° 20' N) cannot be seen in the observed distribution. On the other hand, simulated and observed distributions are in accordance in the southeastern Bay of Biscay and in the three distinct higher concentration areas along the shelf edge from 46 ° 30' N to 45 ° 40' N.

5. DISCUSSION

As current meters measure at a specific point and numerical models give currents representative for an area, i.e. a model grid box, it is common to compare transport rates through a section of a number of moorings to the appropriate section of a number of model points. This was not possible in this case as moorings were located such that no transport rates through a section perpendicular to the shelf edge, i.e. perpendicular to the dominant current direction could be calculated. Thus velocity time series of eularian measurements (current meter) are compared to velocity time series representative for an area of 240.5 km^2 (model). This is one reason for model - measurement discrepancies.

A second important cause for discrepancies between observations and simulations is the horizontal resolution of the windstress fields from ECMWF used in the simulations. These data have a resolution of $1 \times 1°$ which is subsequently interpolated onto the model grid. This horizontal resolution causes a spatial homogeneity of the windstress fields which is not necessarily observed in reality. Small scale fronts, which are linked to strongly fluctuating momentum fluxes at the sea surface (von Storch, 1984) or

mesoscale vortices which give rise to exceptional strong winds (Paulus, 1983) can cause strong currents. These phenomena are not resolved by the windstress field used for the forcing of the circulation model. Thus current peaks in the observations caused by such small scale phenomena will be lacking in the simulated time series.

The third major reason for discrepancies is to be found in the density field used in the simulations. As no quasi - synoptic density fields for the model area and the time under consideration are existent, monthly climatological density fields are used (Levitus, 1982). These data have a resolution of $1 \times 1°$ which is interpolated onto the model grid. Although these data give a good approximation of the monthly density field for the area under consideration, they will nevertheless be different to the real density field for the time period concerned. Different horizontal density gradients and mesoscale eddies are to be expected in the real density field and these will influence the current observations.

Bearing in mind the abovementioned comments, the agreement between observed and modelled currents is good and the discrepancies are mainly caused by local, mesoscale effects which are not resolved by the input data to the circulation model.

The egg/larvae dispersion exercise assumed that 6mm larvae observed during the second cruise derived from the stage I eggs observed during the first cruise, which developed at incubation temperatures of around 12°C (Motos et al., 1996). The available data on hake egg development and hake larval growth rates was revised and forms the basis of this assumption (see section 3c). This assumption is also supported by the small number of larvae larger than 6mm found during the second cruise at 3 stations. These stations coincided with stations where 6 mm larvae were found. It must be noted here that the catchability of plankton nets depends, among other factors, on the size of fish larvae to be caught. Large larvae are more mobile and are able to escape the nets and thus the abundances of large larvae observed during field surveys are generally underestimated (Sherman and Honey, 1971). However, different authors have reported catches of rather large larvae when using BONGO nets. For instance, Olivar et al. (1988) reported 40 cm BONGO catches of Cape hake larvae, Merluccius capensis, up to a length of 16 mm, with a uniformely decreasing frequency histogram from 3mm to 11.5mm and discontinuous catches afterwards. Taking into account the use of 60 cm BONGO nets in the current investigation, it can be expected that larval abundances in the catch are an estimation of the field abundances of larvae until they reach about 10 mm length. Furthermore, small changes in growth rates (eg. 0.04 mm/day) results in a larvae length difference of 1 mm after 25 days. These factors need to be considered when comparing the simulated tracer distributions with the observed 6 mm larvae distributions.

During the second cruise high numbers of 6 mm larvae were found on the two northern sections (fig. 8b). Due to bad weather these two sections, except for four stations, were not sampled on the first cruise. This could imply that a sizeable portion of egg production in this area was missed. Furthermore, egg abundances of stages older than stage I peaked in the northernmost station of the February cruise, showing that there were high egg abundances in the area. These zero stage I egg abundances in

the far north, which are used in the initial distribution in the tracer simulation could, at least in part, account for the discrepancy between larvae observations and tracer distributions in the far north.

The high simulated tracer concentration at the shelf edge (at 45° 20' N) originates from the high egg concentration at 45°N (fig. 10a) which has been dispersed northwestwards along the shelf edge. This high concentration is not evident in the larvae observations and may be due to either enhanced advection onto the shelf in reality, high mortality which is not considered in the transport model or stronger advection along the shelf edge than given by the model system.

The European hake has several known juvenile nursery areas (Anon., 1996). In the Bay of Biscay, a main nursery area is located off the northern coast (Southern Britanny), where hake juveniles (0 group) concentrate from 120m water depth to the coastline from the end of the spring to the autumn (Bez et al., 1995). However, hake eggs in this area in February and March are distributed well offshore mainly over the shelf edge (Motos et al., 1996). Eggs and larvae with their limited active horizontal swimming abilities, must therefore be transported towards the coast over the shelf into the nursery areas. Prevalent residual currents in the area and diffusion processes will determine if the eggs and larvae migrate towards the coast, remain in the spawning areas or are dispersed offshore. Data on recruitment in the Northern Biscay area show that settlement of juvenile hake starts in the outer part of muddy bottoms and that a progressive displacement proceeds towards the inner basin (Guichet, 1988). At any rate, larvae must appear over the platform to have chances of settling onto muddy bottoms and a general transport across the shelf would enable the dispersion into the nursery areas.

The results of the tracer simulation show that northern transport was prevalent in the area in the relevant layers where the eggs and larvae developed (Fig. 9). In addition, it also shows drift onto the shelf (Fig. 10c). These conditions, both northern transport and drift onto the shelf, favour the arrival of hake larvae in coastal areas. In the field data, a patch of 6mm larvae extended over the platform between 46° and 47° 15'N at water depths from 120m to 160m. These larvae are probably approaching the nursery areas which start at 120m water depth (Guichet, 1988).

However, the main patch of 6mm hake larvae is found along and off the shelf edge at 47°N. This larval patch roughly coincides with a mesoscale gyre structure (cyclonic, 70 km diameter) identified in the area (fig. 11). The gyre was located off shelf and velocities were of the order of 10-15 cm/s (Motos et al., 1996). This gyre can entrain outer shelf and shelf edge waters and consequently retain biological material, e.g. fish eggs and larvae or it can advect the biological material towards offshore areas. This mechanism would act against the onshore transport of hake eggs and larvae into nursery areas and can potentially be detrimental for the success of the recruitment.

Another known nursery area is the southeastern corner of the Bay of Biscay at $\sim 2°$W (Sanchez, 1993). There, settlement to the bottom starts in water depths close to 200m and juveniles progressively move towards the 100m depth contour. Afterwards, they

disperse over the nursery area located between 100 and 200m water depth (Farina and Abaunza, 1991; Sanchez, 1993). In this area, a patch of stage I eggs and another patch of 6mm larvae were found in the first and in the second cruise, respectively. This suggests that eggs spawned in February were retained in the area and developed to 6mm larvae by 22 March.

Alternatively, the occurrence of 6mm larvae can result from the accumulation of larvae coming from the coastal areas of the Cantabrian Sea. The general circulation in the area often shows an eastward transport close to the coast and a recurring cyclonic gyre in the southeastern part of the Bay of Biscay. This can result in the accumulation of biological material at the eastern tip of the Cantabrian Sea, where the direction pattern of the currents is variable and the speeds diminish. The general eastward transport and northwesterly wind regime may explain the entrainment of hake larvae on the Cantabrian shelf during winter months (Sanchez, 1993; Cabanas, 1993). This retention process in the southeastern part of the Bay of Biscay was correctly simulated by the model system.

ACKNOWLEDGEMENTS

This research is funded by the European Union under grant Nr. AIR2 - CT93 - 1105. Thanks goes to ECMWF (European Centre for Medium-Range Weather Forecasting) in Reading and the DKRZ (Deutsches Klima Rechenzentrum) for making available the meteorological data for the circulation model. We are grateful to the Spanish Instituto Nacional de Meteorologia for providing us with meteorological time series at Cabo Penas. Adolfo Uriarte and Paula Alvarez collaborated in the processing and analysis of the hake egg and larval cruise data. Finally we would like to thank all SEFOS colleagues who participated directly or indirectly in this investigation for their contribution.

REFERENCES

ANONYMOUS, 1996: Working Group on the Assessment of Southern Shelf Demersal Stocks. ICES C.M. 96/Assess:5.

ALONSO J. and G. DIAZ del RIO, 1996: Current measurements in Cantabrian sea. An analysis of tidal currents (submitted to Oceanologica Acta)

BACKHAUS, J. O., 1985: A three-dimensional model for the simulation of shelf sea dynamics. Deutsche Hydrographische Zeitschrift, 38, Heft 4, 165 - 187.

BACKHAUS, J. O., 1989: On the atmospherically induced variability of the circulation of the Northwest European shelf sea and related phenomena. In: Davies, A. M. (ed.): Modeling Marine Systems, Vol. I. CRC Press, Inc. Boca Raton, Florida, 93 - 134.

BAILEY, K.M., 1981: An analysis of the spawning, early life history and recruitment of the Pacific hake, Merluccius productus. PhD Thesis. University of Washington, 1981.

BAILEY, K.M., FRANCIS, R.C. and P.R. STEVENS, 1982: The life history and fishery of Pacific Whiting, Merluccius productus. CalCOFI Rep., Vol XXIII.

BARTSCH, J., and R. KNUST, 1994a: Simulating the dispersion of vertically migrating sprat larvae (*Sprattus sprattus* (*L.*)) in the German Bight with a circulation and transport model system. Fisheries Oceanography, Vol. 3, Nr. 2, pp. 92 - 105.

BARTSCH, J., and R. KNUST, 1994b: Predicting the dispersion of sprat larvae (*Sprattus sprattus* (*L.*)) in the German Bight. Fisheries Oceanography, Vol. 3, Nr. 4, pp. 292 - 296.

BEZ, N., J. RIVOIRARD and J. Ch. POULARD, 1995: Approche transitive et densites de poissons. Cahiers de Geostatistique 5.

BORK, I. and E. MAIER - REIMER, 1978: On the spreading of power plant cooling water in a tidal river applied to the river Elbe. Advances in Water Resources, 1, 161 - 168.

CABANAS, J.M., 1993: Caracteristicas oceanograficas de la plataforma continental atlantica de la Peninsula Iberica y su pobislbre relaccion con la distribucion de la merluza. In Gonzalez-Garces, A. y Pereiro, F.J. eds. 1994. Jornadas sobre el estado actual delos conocimientos de las poblaciones de merluza que habitan la plataforma continental Atlantica y Mediterranea de la Union Europea con especial atencion a la peninsula Iberica. Publicacion privada, pp. 255-279.

CASARINO B. and L. MOTOS, 1994: Identification and distribution of hake, *Merluccius merluccius*, eggs and larvae in Bay of Biscay waters. Annex to the 1st SEFOS Annual Report. Aberdeen, 1994.

COOMBS, S.H., 1994: Identification of eggs of hake, Merluccius merluccius. J. mar. biol. Ass. U.K., 74: 449-450.

COOMBS, S.H., and MITCHELL, C.E., 1982: The development rate of eggs and larvae of the hake, Merluccius merluccius (L.) and their distribution to the west of the British Isles. L. Cons. int. Explor. Mer. 40: 119-126.

DIAZ del RIO G, J. ALONSO, M.J. GARCIA, J.M. CABANAS and J. MOLINERO, 1992: Estudio dinamico en la plataforma continental del norte de Galicia (Abril-junio 1991). Inf. Tec. I.E.O. Nr. 134, 23 pp.

FARINA, A.C. and ABAUNZA, P., 1991: Contribucion al estudio de los juveniles de merluza entre Cabo Villano y Cabo Prior (NW Galicia) mediante prospecciones pesqueras. Bol. Inst. Esp. Oceanogr. 7 (2): 155-163.

GODIN G., 1991: The analysis of tides and currents. Tidal hydrodynamics. Edited by B. Parker 1991.

GUICHET, R., 1988: Etude de la croissance du merlu europeen (Merluccius merluccius) au cours de ses premiares annees. Analys par NORMSEP des distributions en taille observees trimestriellment en mer de 1980 - 1987. ICES, C.M. 1988/G:53.

INSTITUOT NACIONAL de METEOROLOGIA, 1995: Boletin meteorologico diario, Madrid, February - May 1995.

LEVITUS, S., 1982: Climatological Atlas of the World Ocean. NOAA Technical Paper, 173 pp.

MARRALE D., P. ALVAREZ and L. MOTOS, in press. Early life development and identification of the European hake, Merluccius merluccius L. Ozeanografika (In press).

MOTOS, L., P. ALVAREZ and A. URIARTE, 1996: Spawning of hake, Merluccius merluccius, in the Bay of Biscay in winter 1996. ICES CM 1996/S:8.

OLIVAR, M.P., P. RUBIES and J. SALAT, (1988): Early life history and spawning of Merluccius capensis Castelnau in the northern Benguela Current. S. Afr. J. mar. Sci. 6: 245-254.

PAULUS, R., 1983: Vortex - like cloud structure over the North Sea. Beiträge zur Physik der Atmosphäre, 56, 405 - 406.

PINGREE R.D. and B. Le CANN, 1990: Structure, Strength and Seasonality of the Slope currents in the Bay of Biscay Region. J. mar biol. Ass. U.K. 70, 857 - 885.

POREBSKY, J., 1975: Application of the Surface Adhesion Test to identify the eggs of the hake Merluccius spp. Colln. scient. Pap., Int. Commn. SE Atl. Fish., 2: 102 - 106.

PORTEIRO C., J.M. CABANAS, L. VALDES, P. CARRERA, C. FRANCO and A. LAVIN, 1996: Hydrography features and dynamics of Blue Whiting, Mackerel in the Bay of Biscay. 1994-1996. A multidisciplinary study on SEFOS. ICES C.M. S:13

RUSSELL, F.S., 1976: The eggs and planktonic stages of british marine fishes, London, Academic Press, 524 pp.

SANCHEZ, F., 1993: Patrones de distribucion y abundancia de la merluza en aguas de la plataforma norte de la Peninsula Iberica. In Gonzalez-Garces, A. y Pereiro, F.J. eds. 1994. Jornadas sobre el estado actual delos conocimientos de las poblaciones de merluza que habitan la plataforma continental Atlantica y Mediterranea de la Union Europea con especial atencion a la peninsula Iberica. Publicacion privada, pp. 255-279.

SHERMAN, K. and K.A. HONEY, 1971: Size selectivity of the Gulf III and bongo zooplankton samplers. *ICNAF Res. Bull.*, 8: 45 - 48.

SMITH, P.E. and S.L. RICHARDSON, 1977: Standard techniques for pelagic fish eggs and larval surveys. FAO Fish. Tec. Papers, 175: 100 pp.

STABENO, P. J., HERMANN, N. A., BOND, N. A. and S. J. BOGRAD, 1995: Modeling the impact of climate variability on the advection of larval walleye pollock (*Theragra chalcogramma*) in the Gulf of Alaska. In: Climate Change and Northern Fish Populations, R. J. Beamish (ed.), Can. Spec. Publ. Fish. Aqu. Sci., 121, pp. 719 - 727.

von STORCH, H., 1984: A comparative study of observed and GCM - simulated turbulent surface fluxes at the positions of Atlantic weather ships. Dynamics of Atmospheres and Oceans, 8, 343 - 359.

WERNER, F. E., PAGE, F. H., LYNCH, D. R., LODER, J. W., LOUGH, R. G., PERRY, R. I., GREENBERG, D. A. and M. M. SINCLAIR, 1993: Influences of mean advection and simple behaviour on the distribution of cod and haddock early life stages on Georges Bank. Fisheries Oceanography, Vol. 2, Nr. 2, pp. 43 - 64.

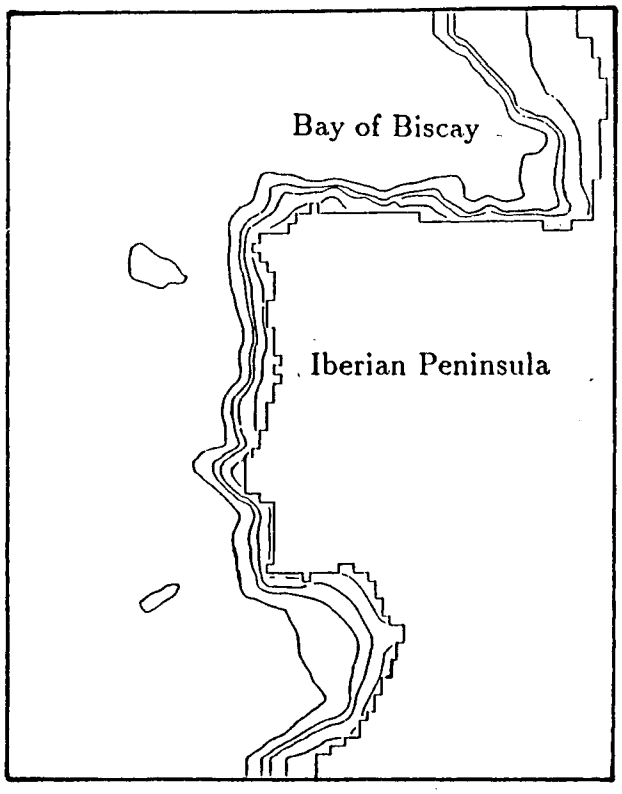

Fig. 1 Southern SEFOS model area and topography showing the 100m, 400m, 800m and 2000m isobaths.

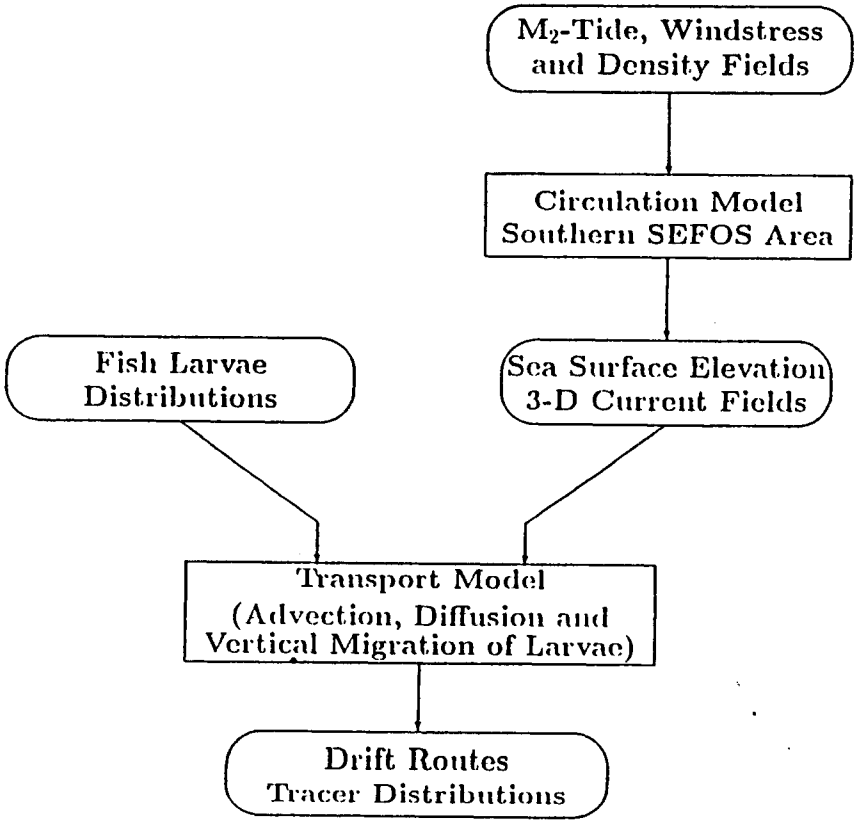

Fig. 2 Schematic diagram of model system. Oval boxes denote input and output data.

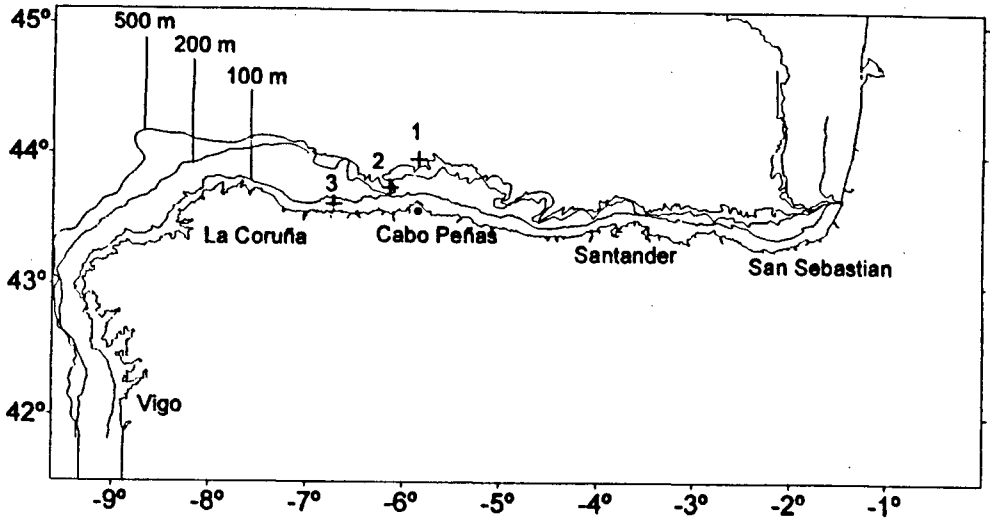

Fig. 3 Location of moorings. Mooring 1 was deployed at 1150 m depth, mooring 2 was deployed at 568 m depth at the shelf break and mooring 3 was deployed at 90 m depth on the continental shelf. The 100 m, 200 m and 500 m isobaths are indicated.

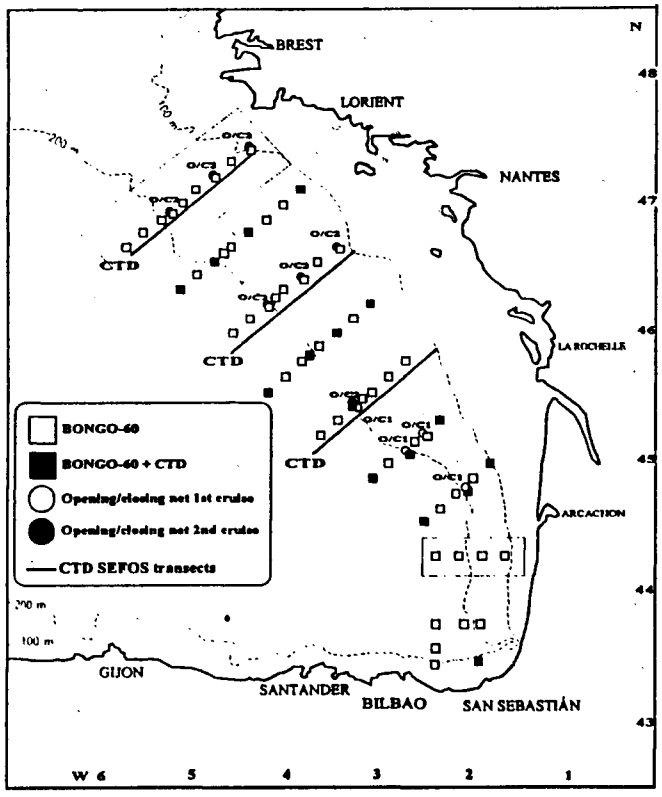

Fig. 4 Sampling grid of the hake egg and larval surveys carried out on board RV INVESTIGADOR in 1995. Two consecutive cruises covered the time periods 15 - 24 February and 22 - 30 March respectively. The same grid was to be covered in both cruises. See legend for details on the sampling scheme. Areas surrounded by closed lines were not covered during the February cruise.

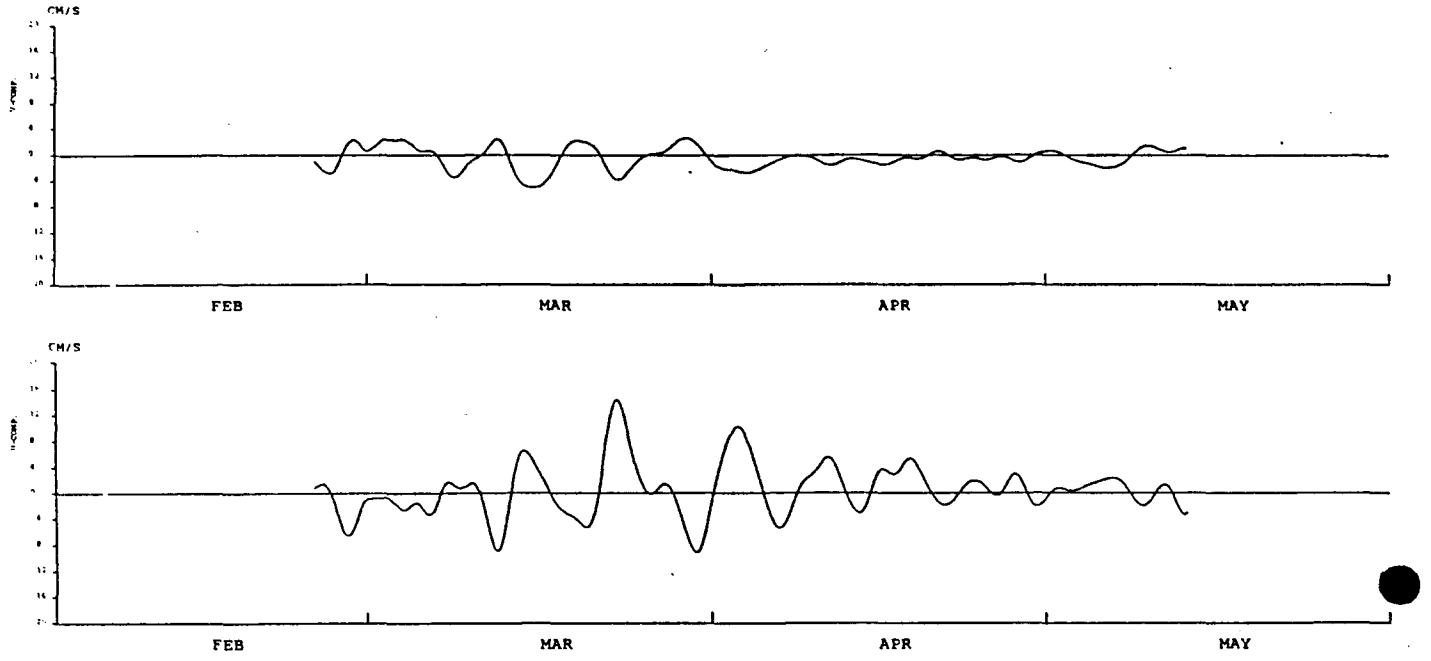

Fig. 5 a) Observed current components (u bottom, v top) at mooring 3 (74 m) between February - May 1995.

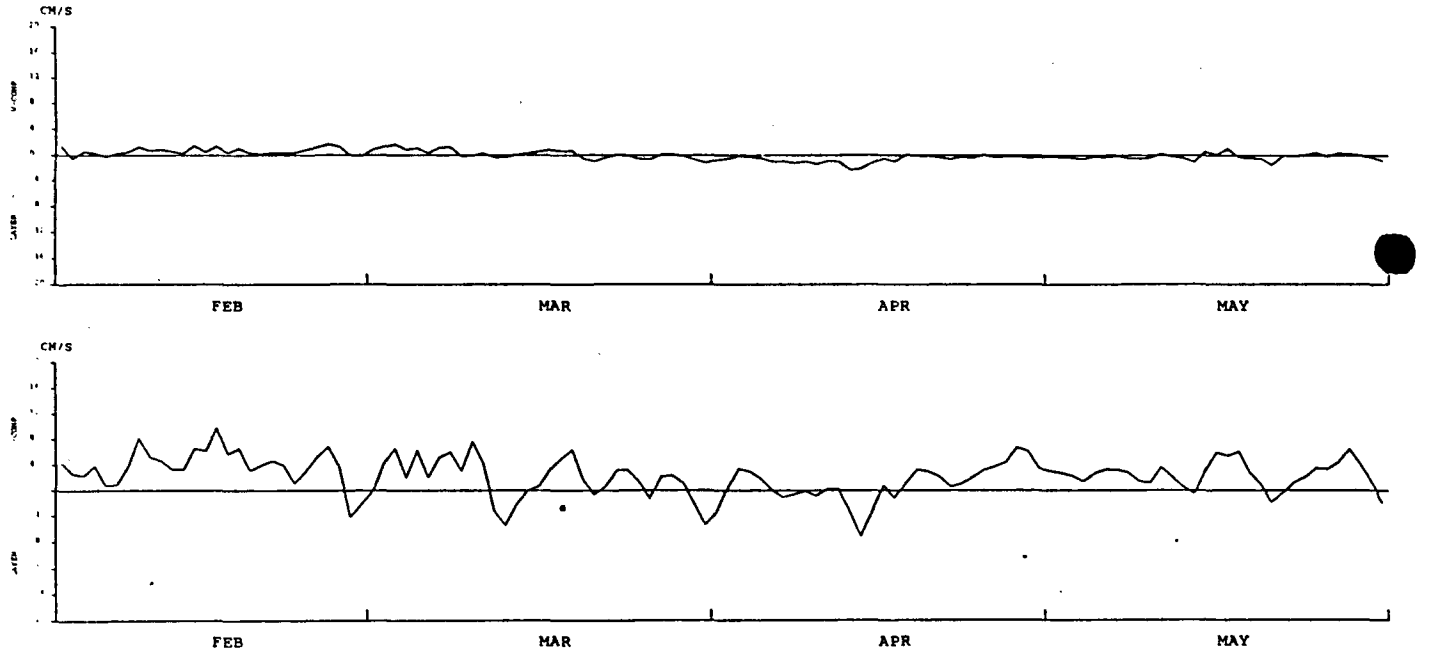

Fig. 5 b) Simulated current components (u bottom, v top) at mooring 3 in model layer 5 (80 m) between February - May 1995.

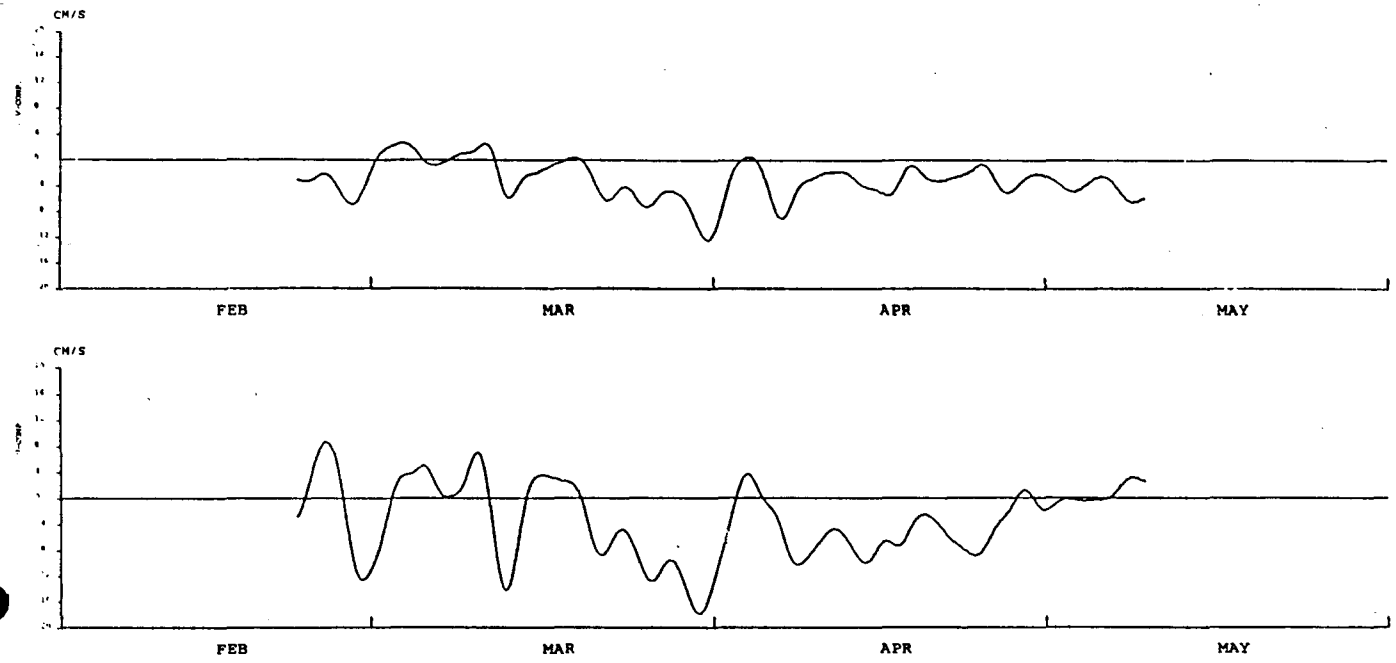

Fig. 6 a) Observed current components (u bottom, v top) at mooring 2 (80 m) between February - May 1995.

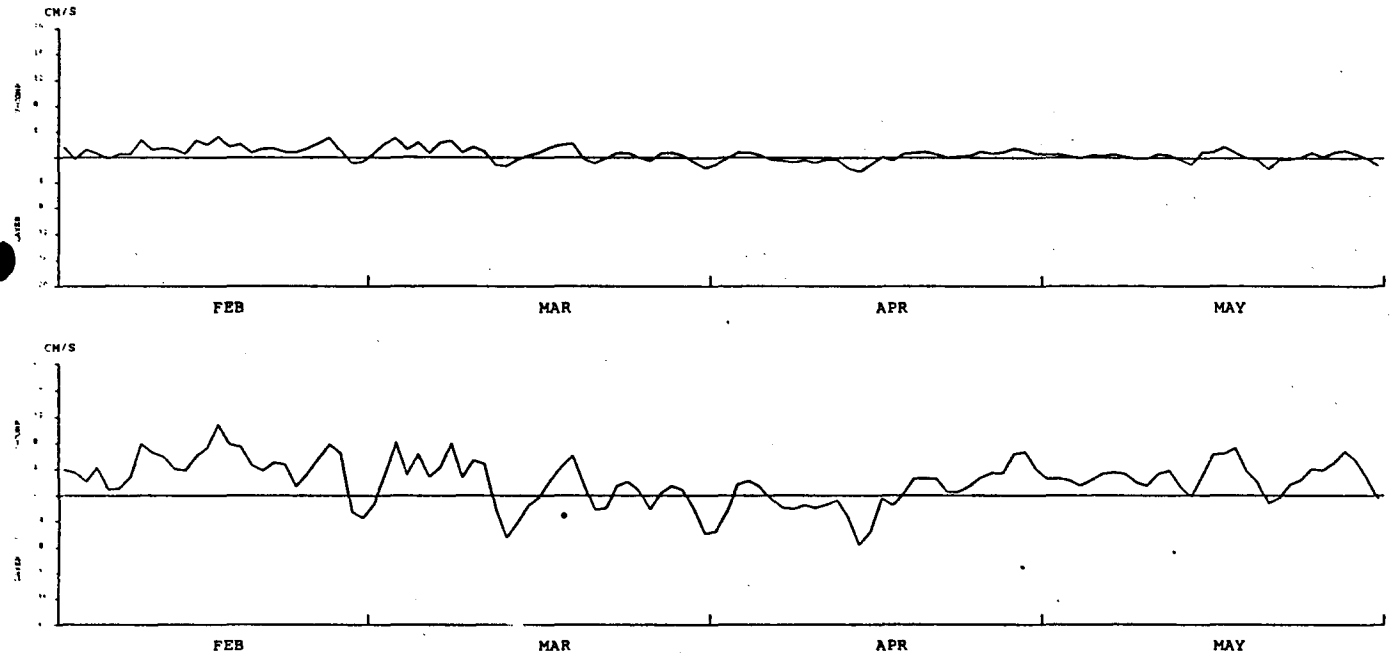

Fig. 6 b) Simulated current components (u bottom, v top) at mooring 2 in model layer 5 (80 m) between February - May 1995.

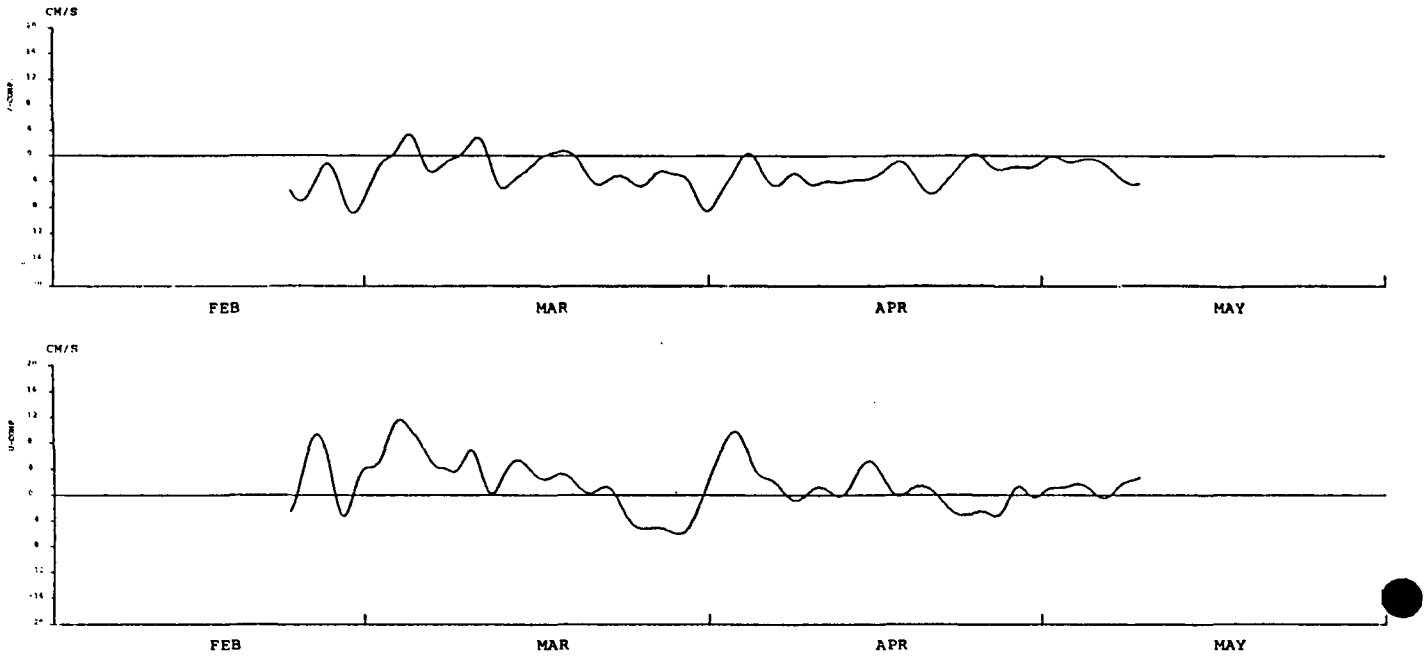

Fig. 7 a) Observed current components (u bottom, v top) at mooring 2 (180 m) between February - May 1995.

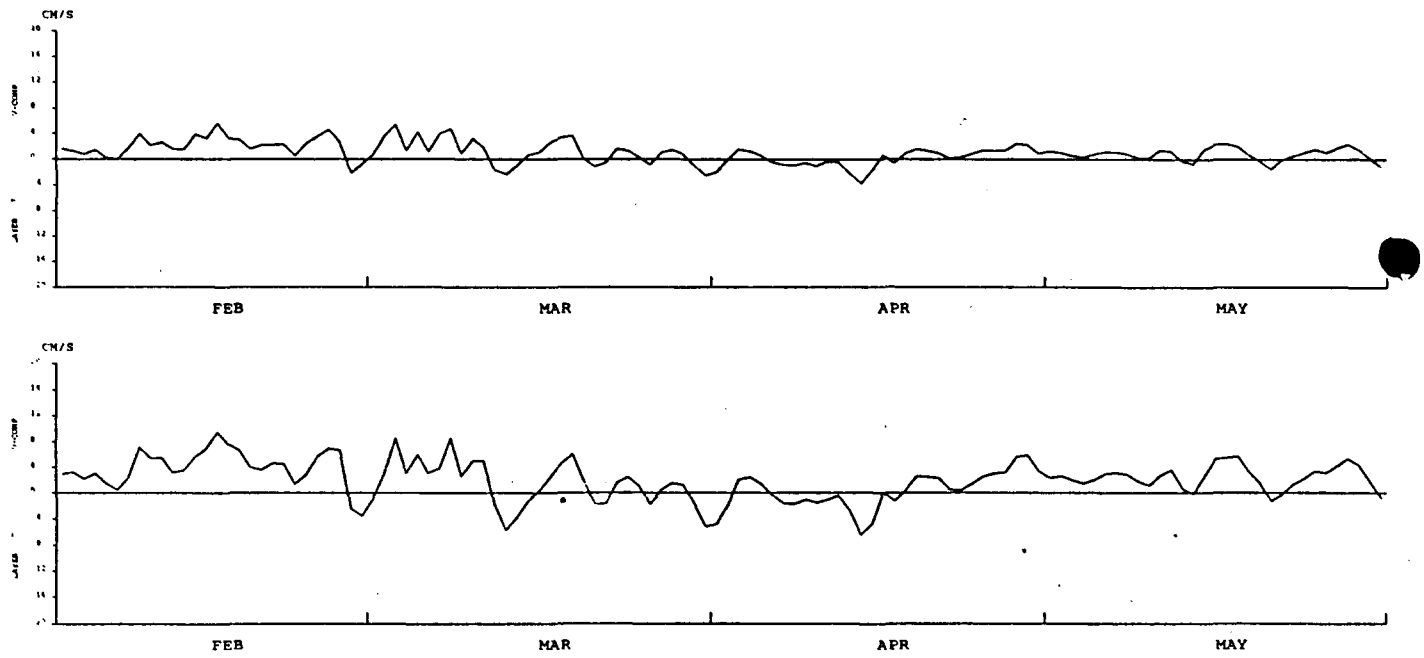

Fig. 7 b) Simulated current components (u bottom, v top) at mooring 2 in model layer 7 (175 m) between February - May 1995.

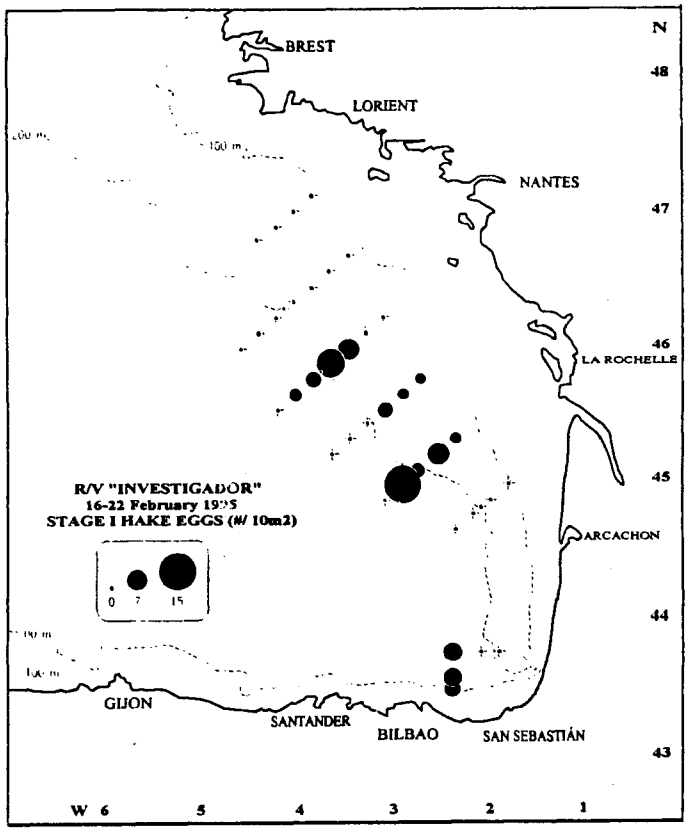

Fig. 8a: Hake stage I egg abundances found during the survey period 16-22 February 1995 (mid date: 19 February). Egg abundances are given in numbers per 10m².

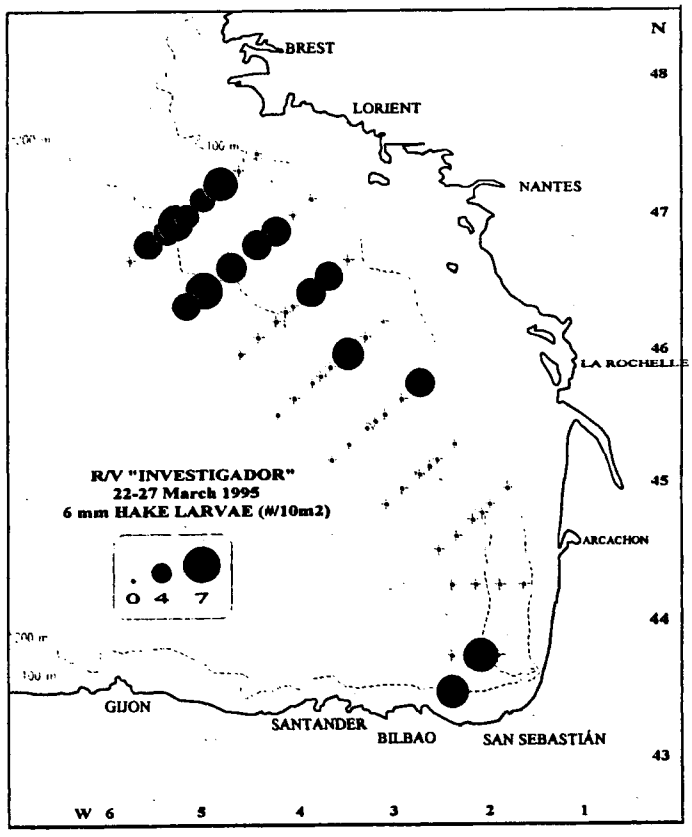

Fig. 8b: Abundances of 6 mm hake larvae found during the survey period 22-27 March 1995 (mid date: 25 March). Larval abundances are given in numbers per 10m².

9 b)

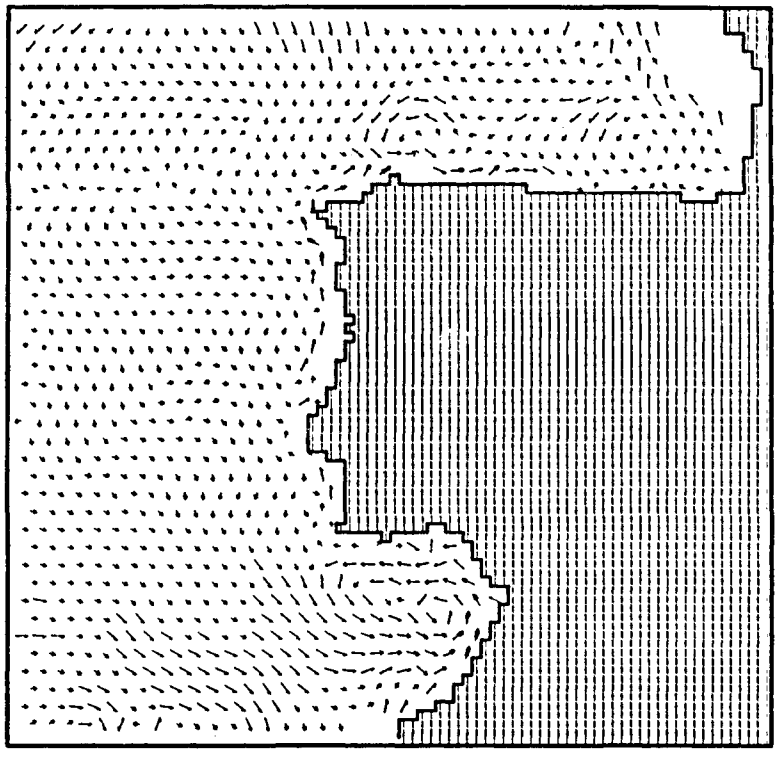

9 a)

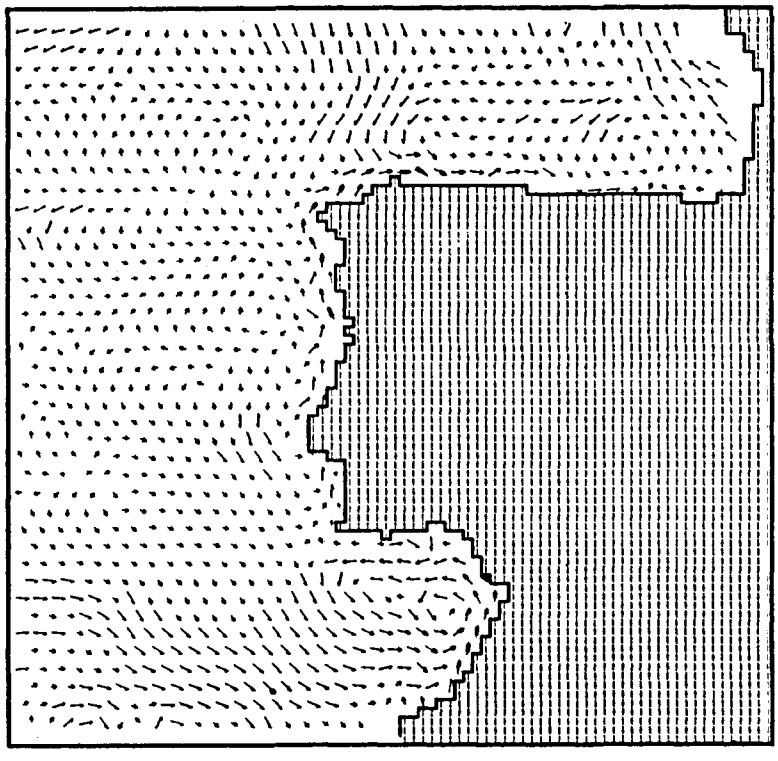

Fig. 9 Simulated circulation field on 10. 3. 1995 in model layer 5 (80m, (a)) and in model layer 6 (125m, (b)). Smallest arrows denote speeds < 2 cm/s. As arrow size increases, current speeds increase by 2 cm/s increments.

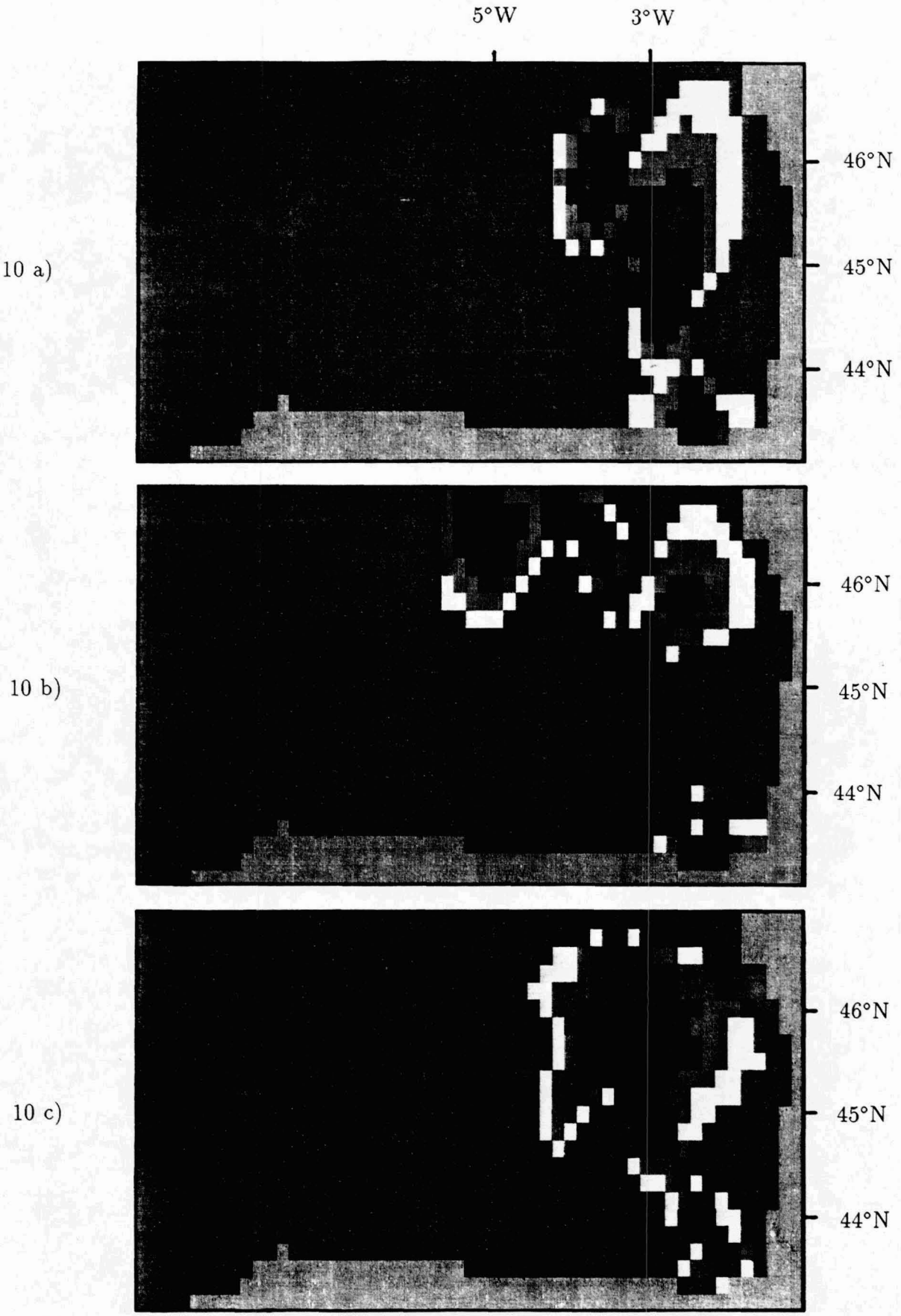

Fig. 10 a) Observed hake egg (stage Ia and Ib) distribution in the Bay of Biscay on 17 February 1995 interpolated onto the model grid. Initial distribution of tracer simulation.

Fig. 10 b) Observed hake larvae (6 mm) distribution in the Bay of Biscay on 27 March 1995 interpolated onto the model grid.

Fig. 10 c) Simulated tracer distribution after 39 days dispersion in the Bay of Biscay on 27 March 1995.

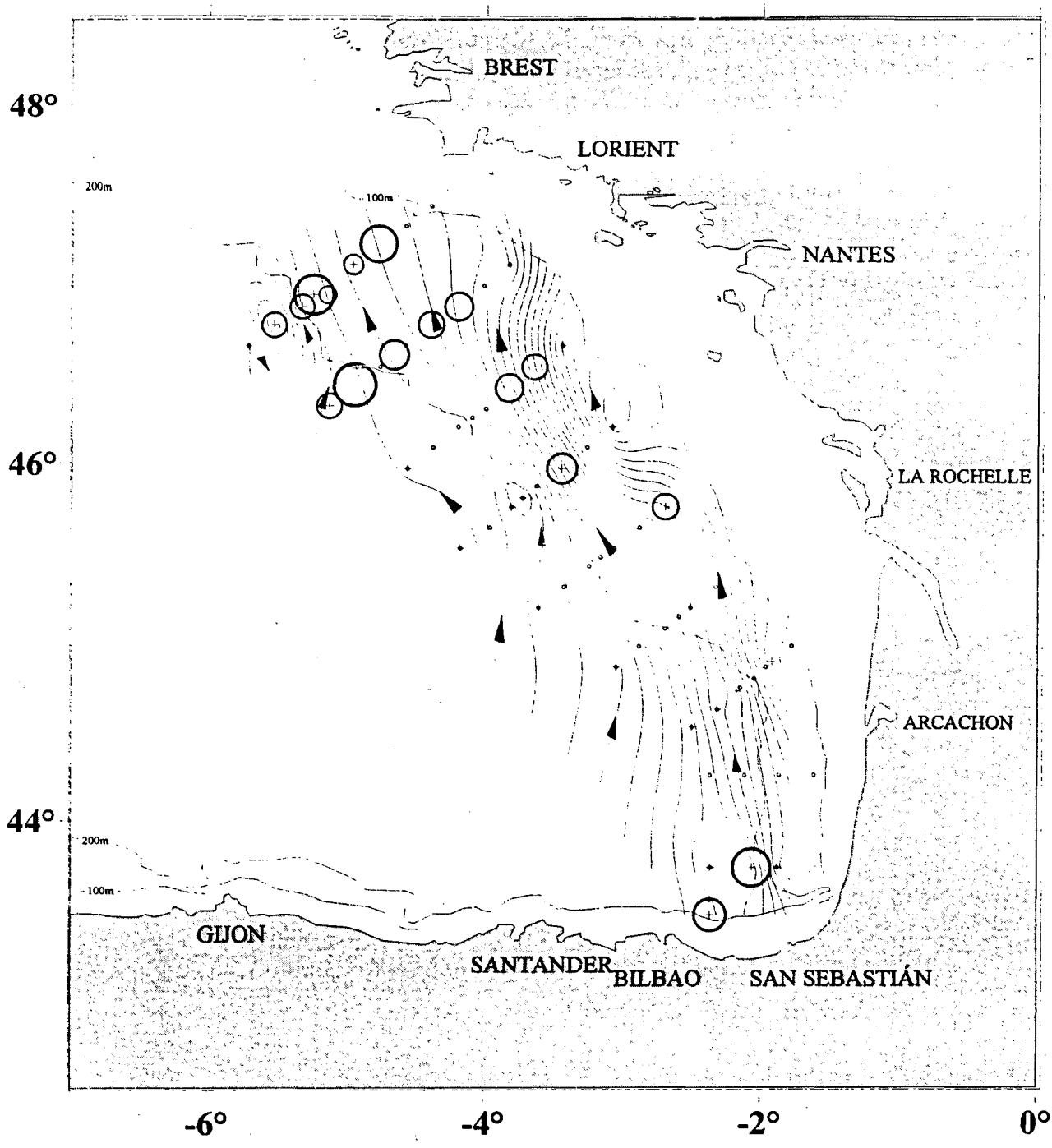

Fig. 11: Dynamic heights (0.2cm intervals) from 10/100 dbars, indicating the general geostrophic circulation (arrows) during the period 22-27 March 1995. Open circles illustrate the abundance of 6mm hake larvae (the biggest circle represents 7 individuals of the 6mm lenght class per 10 m^2).

Table 1: Summary of the information available on the egg development and larval growth rates of hake. Values in the table are time (in days) to reach the different developmental stages: Hatching, end of yolk-sac larva and different sizes of post-larva. In the latter, G refers to the Gompertz curve fit and L to the linear fit to observed larval growth figures (Bailey, 1981). This author pointed out that larval growth was better explained by a linear increment of 0.16 mm d^{-1} up to approximately the 32nd day of live. In italics, time to the end of the yolk-sac larval stage assuming that the growth pattern of *M. merluccius* at this stage is similar to that of *M. productus*. See text.

		Merluccius productus - Bailey (1981)					M. merluccius - Coombs & Mitchell (1982)				
temperature		**10**	**11**	**12**		**13**	**15**	**10**	**11**	**12**	**13**	**15**
hatching		5.28	4.81	4.40		4.05	3.49	6.82	5.96	5.27	4.71	3.85
end of yolk-sac larva		14.68	12.73	11.08		9.68	7.50	*16.47*	*14.09*	*12.12*	*10.49*	7.96
	length			G	L					G	L	
post-larva	4 mm			22	18					23	19	
	5 mm			26	24					27	25	
	6 mm			30	31					31	32	
	7 mm			33	37					34	38	
	8 mm			36	43					37	44	